Eddy PV Fluxes in a One Dimensional Model of Quasi-Geostrophic Turbulence

Christos M.Mitas

1 Introduction

1.1 Motivation

Understanding eddy transport of heat and momentum is crucial to developing closure schemes for general circulation models.

While eddy momentum fluxes do not adhere to a clear parameterization methodology, potential vorticity (PV) and heat fluxes may be easier to comprehend and thus parameterize.

If the eddy diffusivity (defined as the eddy flux over the mean gradient) was computed from a simple homogeneous model, it could be fit with an analytic function of the various model parameters, and subsequently used in a inhomogeneous model to provide closure for the zonal mean quantities that are forced by eddy fluxes.

1.2 Problem Formulation

Highly idealized baroclinic models have been frequently used to study various aspects of homogeneous turbulence ([1, 2, 3, 4]). These studies used doubly periodic, two-layer, quasi geostrophic models on a β plane to represent the interior of a channel flow that is continuously forced by an imposed vertical shear (U). The use of a doubly periodic box is enforcing the homogeneity of the turbulent flow. In both [3] and [4] the eddy statistics of the equilibrated flow do not appear to depend on the length of the domain, thus the representation of the channel interior seems to be accurate.

To achieve computational economy and at the same time retain essential features of homogeneous turbulence, [4] in their study of baroclinic eddy fluxes have used a truncated model. This model retains only the zonally averaged flow and one nonzero wavenumber in the zonal direction, but has high meridional resolution to allow for an enstrophy cascade. Severely truncated models have been used in numerous meteorological studies, for diverse topics as sudden stratospheric warmings ([5]) and climate sensitivity ([6]), among others.

In this project a doubly periodic, quasi geostrophic, two-layer model, with a rigid lid and flat bottom, truncated in the zonal direction and with high resolution in the meridional direction is implemented and used to assess eddy fluxes.

2 Methodology

2.1 The Two Layers, Doubly Periodic, QG Model

2.1.1 Equations

In the formulation of the model we follow [4] . The layers are of equal depth H. A rigid lid on top and a bottom horizontal surface defines the vertical boundaries. The Coriolis parameter is f_0. The meridional coordinate y measures distance from the domain center. Subscripts 1 and 2 refer to the upper and lower layer, respectively. The internal Rossby radius of deformation is defined by $\lambda^2 = g(\rho_2 - \rho_1)H/(2\rho_2 f_0^2)$. Ekman friction is implemented only for the lower layer. A scale-selective biharmonic diffusion of potential vorticity is included to absorb the enstrophy cascade. The friction and diffusion coefficients are denoted by κ and ν respectively.

The dimensional equations in terms of the streamfunctions Ψ_j read:

$$\frac{\partial Q_1}{\partial t} + J(\Psi_1, Q_1) = -\nu\nabla^4 Q_1 \tag{1}$$

$$\frac{\partial Q_2}{\partial t} + J(\Psi_2, Q_2) = -\nu\nabla^4 Q_2 - \kappa\nabla^2\Psi_2 \tag{2}$$

where the potential vorticity Q_j is:

$$Q_j = \beta y + \nabla^2\Psi_j + (-1)^j(\Psi_1 - \Psi_2)/(2\lambda^2), \quad j = 1, 2$$

We now assume that there is a positive vertical shear U and that the upper and lower layer streamfunctions are given by:

$$\Psi_1(x, y, t) = -\frac{U}{2}y + \psi_1(x, y, t)$$

$$\Psi_2(x, y, t) = +\frac{U}{2}y + \psi_2(x, y, t)$$

We non-dimensionalize (x, y, t, ψ_j) with $(\lambda, \lambda, \lambda/U, U\lambda)$. It follows that the dimensionless parameters are $\hat{\beta} = \beta\lambda^2/U$, $\hat{\kappa} = \kappa\lambda/U$, and $\hat{\nu} = \nu/(U\lambda^3)$.

If we drop the hats in the dimensionless parameters the eddy equations become:

$$\frac{\partial q_j}{\partial t} + J(\psi_j, q_j) = F_j + D_j \tag{3}$$

The transient eddy potential vorticities are given by:

$$q_j = \nabla^2\psi_j + (-1)^j\tau$$

where $\tau = (\psi_1 - \psi_2)/2$ is the baroclinic perturbation that is proportional to the vertical thickness. The right-hand-side terms represent forcing by the imposed mean flow,

$$F_1 = -\frac{1}{2}\frac{\partial q_1}{\partial x} - (\beta + 1/2)\frac{\partial \psi_1}{\partial x}$$

$$F_2 = +\frac{1}{2}\frac{\partial q_2}{\partial x} - (\beta - 1/2)\frac{\partial \psi_2}{\partial x}$$

and dissipation by Ekman friction and hyper-diffusion:

$$D_1 = -\nu\nabla^4 q_1$$

$$D_2 = -\nu\nabla^4 q_2 - \kappa\nabla^2\psi_2$$

To retain only the zonal mean and a nonzero wavenumber k in the x-direction, we assume that the streamfunctions ψ_j are of the form:

$$\psi_j(x, y, t) = \psi_{j,0}(y, t) + (\psi_{j,k}(y, t)e^{ikx} + c.c.) \tag{4}$$

where the $\psi_{j,0}(y, t)$ is referred as the "zonal mean component" and the $\psi_{j,k}(y, t)$ as the "wave component". If we further ignore wave-wave interactions (i.e. the e^{2ikx} waves), the resulting equations for the two components are:

$$\frac{\partial q_{j,0}}{\partial t} = -2Re\frac{\partial(ik\psi_{j,k}q^*_{j,k})}{\partial y} \tag{5}$$

$$\frac{\partial q_{j,k}}{\partial t} = ik(q_{j,k}\frac{\partial \psi_{j,0}}{\partial y} - \psi_{j,k}\frac{\partial q_{j,0}}{\partial y}) \tag{6}$$

where an asterisk denotes complex conjugation, and the decomposition of q_j, F and D is as in (4).

2.1.2 Numerical Solution

We choose to solve the real equation (5), and complex equation (6) using spatial finite differencing and a leapfrog scheme for the time differencing. Inspection of the equations suggest that the zonal mean and wave components should be staggered with respect to each other so that the y-derivatives would be computed with the smallest error. Note that with this type of staggering, the non-linear terms, corresponding to the Jacobians in equation (3) exactly conserve enstrophy and energy.

$\hat{L}$ is the non-dimensional parameter controlling the length of the domain that is set to $2\pi\hat{L}$. All the experiments reported here have used $\hat{L} = 10$. The number of grid points in the y-direction is set to $N = 256$. With this choice for $\hat{L}$ and N, the meridional wavenumber is given by: $l_n = n/L, n = 1 \cdots N/2$, where n is the discrete meridional wavenumber. Thus, the grid spacing is $dy =\sim 0.245$ (i.e. ~ 4 points per internal radius of deformation), which appears to be adequate to resolve baroclinic eddies in our model.

2.1.3 Spectra

Following [4] again, we calculate spectra for the various quantities in our model (enstrophy q_j^2, kinetic energy $\frac{1}{2}(u_j^2+v_j^2)$, potential energy $\frac{1}{2}\tau^2$, etc.) as follows: If the Fourier coefficients of the zonal mean components of two functions f, g are $F_{0,n}$, $G_{0,n}$ and those of their wave components are $F_{k,n}$, $G_{k,n}$, then the spectrum $\{z_n\}$ of zonal component of $< fg >$ is defined as:

$$z_n = 2c_n Re(F_{0,n}G^*_{0,n}), \quad n = 1, \cdots, N$$

and the spectrum $\{w_n\}$ of the wave component as:

$$w_n = 2c_n Re(F_{k,n}G^*_{k,n} + F_{k,-n}G^*_{k,-n}), \quad n = 0, \cdots, N$$

where c_n is $\frac{1}{2}$, if $n = 0$ or $n = N$, and is 1, otherwise.

2.2 Modal Variables Formulation

An alternative representation of the two layers system may be formulated in terms of the so-called modal variables defined as: $\psi = (\psi_1 + \psi_2)/2$ and $\tau = (\psi_1 - \psi_2)/2$, where ψ and τ are identified as the barotropic and baroclinic streamfunctions, respectively.

The non-dimensional equations are modified as follows:

$$\frac{\partial \nabla^2\psi}{\partial t} + J\big(\psi, \nabla^2\psi\big)\big) + J\big(\tau, \nabla^2\tau\big)\big) = -\frac{1}{2}\frac{\partial \nabla^2\tau}{\partial x} - \beta\frac{\partial \psi}{\partial x} - \frac{\kappa}{2}\nabla^2(\psi - \tau) - \nu\nabla^4(\nabla^2\psi) \quad (7)$$

$$\{\frac{\partial \nabla^2\tau}{\partial t} + J\big(\psi, \nabla^2\tau\big)\big) + J\big(\tau, \nabla^2\psi\big)\big)\} - \frac{\partial \tau}{\partial t} - J(\psi, \tau) =$$
$$\{-\frac{1}{2}\frac{\partial \nabla^2\psi}{\partial x} - \beta\frac{\partial \tau}{\partial x} - \frac{\kappa}{2}\nabla^2(\tau - \psi) - \nu\nabla^4(\nabla^2\tau)\} - \frac{1}{2}\frac{\partial \psi}{\partial x} + \nu\nabla^4\tau \quad (8)$$

The corresponding dimensional equations on an f-plane may be found in [7].

For ease of reference we define barotropic and baroclinic vorticities as $\zeta = \nabla^2\psi$, $\phi = \nabla^2\tau$, respectively, and the baroclinic potential vorticity as $\rho = \nabla^2\tau - \tau = \phi - \tau$. Note that the barotropic vorticity and potential vorticity are identical.

The equations for the barotropic and baroclinic zonal mean components become:

$$\begin{aligned}\frac{\partial \zeta_0}{\partial t} &= -2\frac{\partial Re(ik(\psi_k\zeta^*_k + \tau_k\phi^*_k))}{\partial y} \\ &\quad -\frac{\kappa}{2}(\zeta_0 - \phi_0) \\ &\quad -\nu\nabla^4\zeta_0 \end{aligned} \quad (9)$$

$$\begin{aligned}\frac{\partial \rho_0}{\partial t} &= \{-2\frac{\partial Re(ik(\psi_k\phi^*_k + \tau_k\zeta^*_k))}{\partial y}\} + 2\frac{\partial Re(ik(\psi_k\tau^*_k))}{\partial y} \\ &\quad \{-\frac{\kappa}{2}(\phi_0 - \zeta_0)\} \\ &\quad -\nu\nabla^4(\{\phi_0\} - \tau_0) \end{aligned} \quad (10)$$

The equations for the barotropic and baroclinic wave components read:

$$\begin{aligned}\frac{\partial \zeta_k}{\partial t} &= -ik(\psi_k\frac{\partial \zeta_0}{\partial y} - \zeta_k\frac{\partial \psi_0}{\partial y} + \tau_k\frac{\partial \phi_0}{\partial y} - \phi_k\frac{\partial \tau_0}{\partial)}y \\ &\quad -ik(\frac{1}{2}\phi_k + \beta\phi_k) \\ &\quad -\frac{\kappa}{2}(\zeta_k - \phi_k) \\ &\quad -\nu\nabla^4(\zeta_k e^{ikx}) \end{aligned} \quad (11)$$

$$\begin{aligned}\frac{\partial \rho_k}{\partial t} &= \{-ik(\psi_k \frac{\partial \phi_0}{\partial y} - \phi_k \frac{\partial \psi_0}{\partial y} + \tau_k \frac{\partial \zeta_0}{\partial y} - \zeta_k \frac{\partial \tau_0}{\partial y}\} + ik(\psi_k \frac{\partial \tau_0}{\partial y} - \tau_k \frac{\partial \psi_0}{\partial y}) \\ & \{-ik(\frac{1}{2}\zeta_k + \beta\tau_k)\} - \frac{1}{2}ik\psi_k \\ & \{-\frac{\kappa}{2}(\phi_k - \zeta_k)\} \\ & -\nu\nabla^4((\{\phi_k\} - \tau_k)e^{ikx})\end{aligned} \tag{12}$$

Note that the modal formulation is exactly equivalent in terms of truncation, domain size, numerics, conservation laws, and non-dimensionalization to the two-layer formulation. The reason for the re-formulation of the model will be discussed in the next section when we describe a reduced model derived from the modal variables model.

The non-dimensional parameters of the model are still β (which may be thought as the inverse of supercriticality $\xi = (U/\lambda^2)/\beta$) and the frictional parameter κ. Inviscid instability occurs when $\beta < 0.5$. The most unstable wavenumber is $k = \sqrt{2}/2$, which is the retained wavenumber in the calculations presented here. The model has been integrated for 1100 non-dimensional time units for various parameter configurations. The initial conditions had small amplitudes in all the retained wavenumbers. Note that a time unit is λ/U; if we choose realistic values for the internal radius of deformation ($\lambda \sim 10^6 m$) and the mean vertical shear ($U \sim 10 m/s$) we estimate a time unit to be about 1 day.

In this report, results from the modal variables model are presented. Figure (1) shows the experiments that were performed for various choices of β and κ.

Figure (2) presents a table of plots of the time series of the total energy in the model for the days of integration. Note that equilibration is reached around the 600th time unit. Generally, the equilibration energy level is higher for high values of supercriticality, as expected. It appears that lower values of friction do not signify higher PV flux, a point that we return later.

Figure (3) presents a table of plots of the time series of the PV flux in the model for the integration period. For high values of supercriticality and low friction, the PV flux seems to be fluctuating greatly. Friction seems to decrease the PV flux variance, but not affect its amplitude greatly.

In Figure (4) the energy spectra are displayed for a two experiments with varying β and κ. If the scale of the domain was the largest scale of the flow, one would expect the wave energy spectra to strongly peak at $l = 0$. Clearly, this is not the case for these particular choices of parameters. Note that the most energetic scale of the zonal mean component is not at the radius of deformation (discrete wavenumber $n = 10$, or $l_n = 1$) but at smaller scales around $n = 5$ ($l_n = 0.5$).

The Hovmuller diagrams for the same parameters choices are displayed in (5) computed at longitude $x = 0$. The turbulent nature of the flow is clearly evident. Also evident are zonal jets that persist for long periods. The less supercritical experiment has smaller streamfunction amplitude although the friction is half of the more supercritical one.

Figure (6) shows the spectra of PV flux for four experiments with varying β while the friction held at $\kappa = 0.2$. Similarly, Figure (7) shows the spectra of PV flux for three experiments with varying κ while β is held at 0.15. The PV flux spectra vary significantly for different values of supercriticality, while they do not appear to fluctuate greatly for varying friction.

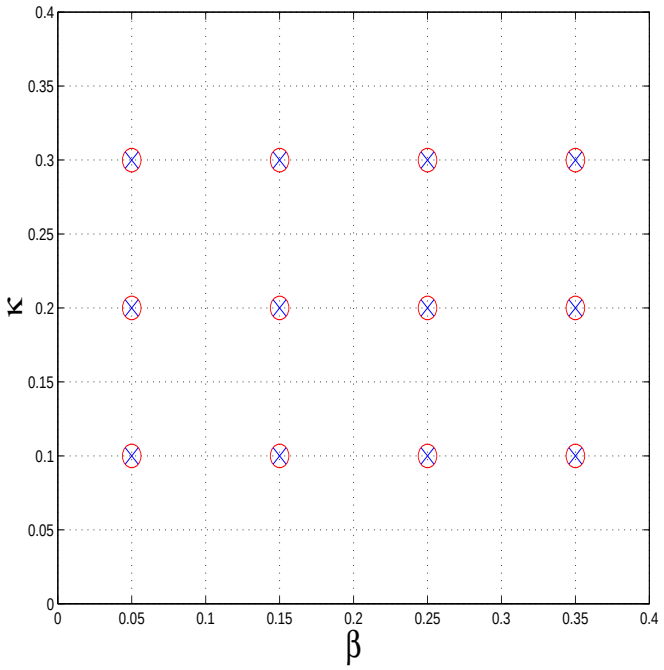

Figure 1: Performed integrations for varying β and κ. The retained zonal wavenumber is $k = \sqrt{2}/2$, the length of the domain is given by $L = 10$ and the hyper-diffusion coefficient is set to $\nu = 10^{-3}$

2.3 Reduced Model

[2] argued that the large-scale motion of the two layers system is dominated by the barotropic streamfunction ψ, while the baroclinic streamfunction τ acts as a passive tracer, and cascades downscale towards smaller scales. The same line of argument has been pursued in [7, 8] to provide scaling arguments for the PV flux. The baroclinic mode is assumed to be mixed downgradient by the turbulent diffusion provided by the barotropic flow.

To test this hypothesis we drop the terms in curly brackets from equation (8), (correspondingly from equations (10) and (13)) and solve the reduced system of equations.

The reduced system needs a rather drastic modification in the value of eddy viscosity that is applied to the baroclinic and barotropic wave components. The eddy viscosity applied to the zonal mean components is the same as in the full model.

This is necessary to prevent an "ultraviolet catastrophe", where the smaller meridional scales are more unstable than the larger ones. The linear growth rate of the full system along with linear growth rates of the reduced system modified by an eddy viscosity term of varying order are displayed in Figure 8. We choose to use a second order diffusion operator with a value of 0.280 for ν. This type of eddy viscosity appears to provide the best fit of the full model's linear growth rate.

The time series of the total kinetic energy, PV flux, and the kinetic energy of the zonal and wave components for each layer for the full and reduced models are shown in Figure 9. It seems that the reduced model is not able to quantitatively capture the essential physics of the full model. Its PV flux is much lower (almost half) than the full model. The total

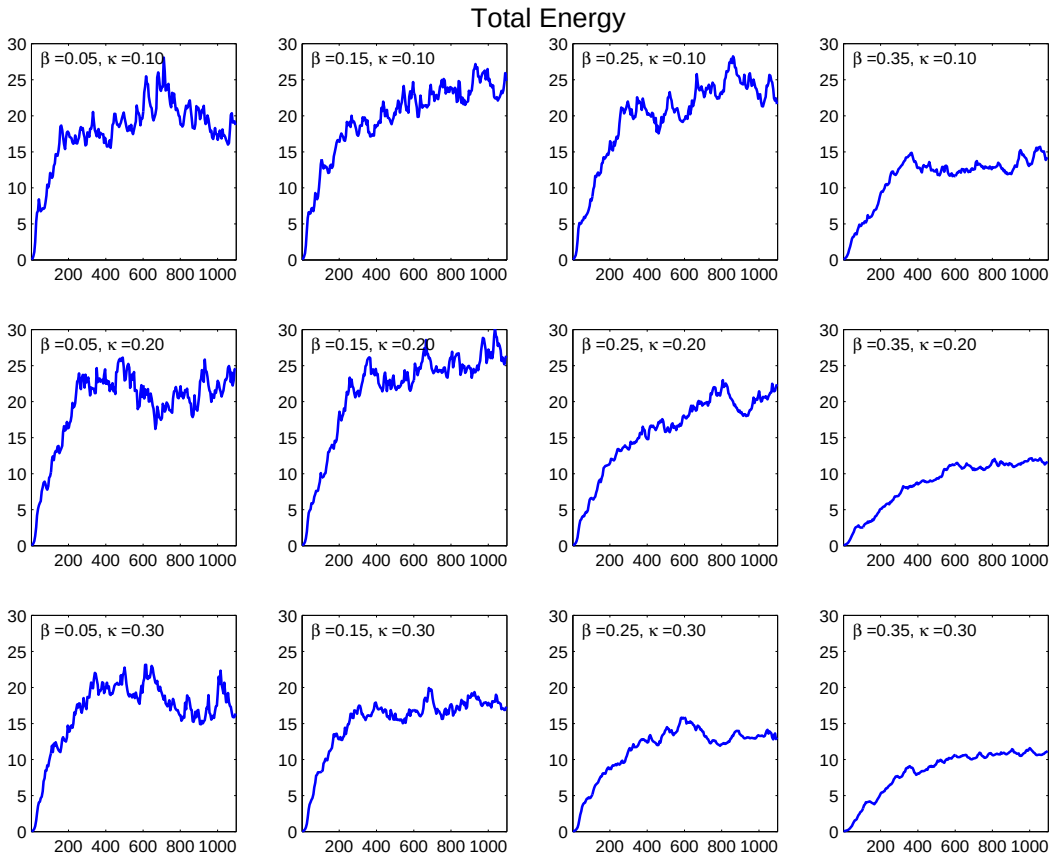

Figure 2: Table of time series of total energy for the integration period.

energy never increases to the level of the full model, mainly because the upper layer kinetic energy remains very low. This seem to be a side effect of the eddy viscosity that we use in our attempt to parameterize the neglected terms of the full model. Clearly, more effort needs to be put in quantitatively using a reduced model like ours.

3 Sensitivity Experiments

Several experiments were performed spanning a moderate area of the parameter space (see Figure 1). The objective of the multiple runs is to gain an overview of the behavior of the PV flux for different choice of parameters.

Figures 10 and 11 display the computed time averaged PV flux for various choices of β and κ.

An interesting feature of the PV flux dependence on friction is shown in 11. There is a local maximum in PV flux around $\kappa = 0.20, 0.15$. The decreasing fluxes for increasing κ may be readily understood as the direct effects that friction has on the energy that is transported in the system. However, the decrease in PV flux for decreasing κ may be understood in different terms. The equilibrated system experiences barotropic eddies that the size depends

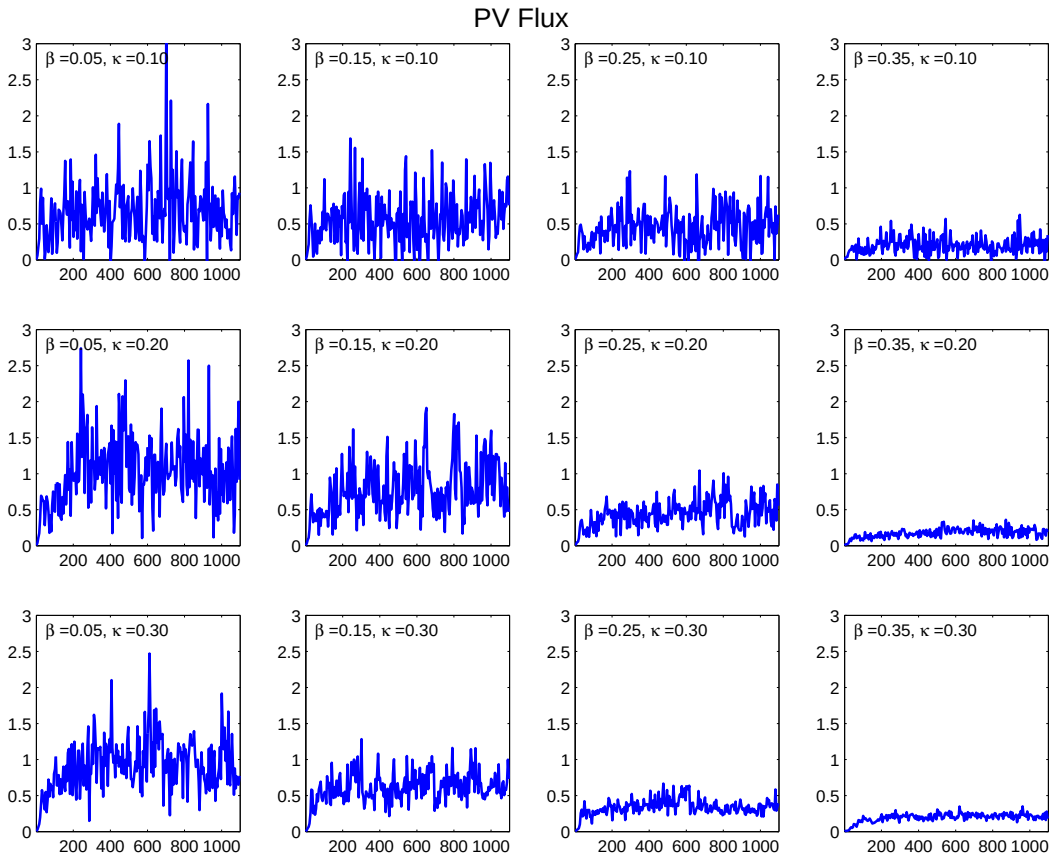

Figure 3: Table of time series of PV flux for the integration period.

on their frictional dissipation. [2] has hypothesized that these barotropic eddies strain the unstable baroclinic eddies so that their meridional wavenumber becomes very large and their linear growth rate decreases. Weaker friction will permit the barotropic energy to cascade to large barotropic eddies (mainly zonal) that are less efficient in providing PV fluxes, while they will strain all the smaller baroclinic eddies. Thus, the local maximum in PV flux would correspond to a value of the frictional parameter κ for which the straining of the unstable baroclinic eddies is not as efficient and the transport accomplished by the barotropic eddies is not small. It appears that for higher β (i.e. lower supercriticality) the local maximum is shifted towards lower κ's indicating that the straining mechanism hypothesized above is performed by the large barotropic eddies left by friction in the system, at sizes larger than their counterparts in a more supercritical system.

As expected, Figure 10 shows that the PV flux generally increases with decreasing non-dimensional β (i.e. increasing supercriticality). The same type of result has been presented in [4] (their Figure 4d) and has been added here for comparison. Some interesting behavior is displayed at intermediate values of β when κ is 0.1 and 0.3. This may be understood in terms of the behavior that the eddies have been hypothesized to acquire in the above paragraph.

4 Conclusions and Future Work

In this work we use a quasi-geostrophic, two-layer model, severely truncated in the zonal direction, to understand the eddy PV fluxes. To ascertain homogeneity, a doubly periodic boundary condition was used. To enable an inertial range of enstrophy cascade, a large resolution is kept in the meridional direction. The system then equilibrates by reducing the northward heat flux $< \psi_x \tau >$, i.e. the correlation of the northward velocity with temperature, and by non-linear transfer of energy from unstable baroclinic waves to stable ones (or less unstable) through triad interactions and consequent frictional dissipation ([2]).

It was also attempted to reduce the model to one that has guided many qualitative arguments (e.g. [7], [2]) concerning the parameterization of eddy PV fluxes. Unfortunately, quantitative use of this kind of reduced system does not appear to be fruitful. To avoid an "ultraviolet catastrophe" in the reduced model, where the waves with larger wavenumber grow the fastest, the eddy viscosity assumes the role of the neglected terms to stabilize the large wavenumbers. In this case, the gross statistics of the reduced model do not resemble the ones of the full model. It may be possible, that another way of preventing the smaller waves to grow without bound exists, in which case the reduced model may be revisited.

The eddy PV flux in our system appears to depend only marginally on the frictional parameter κ. An interesting behavior, where there is a local maximum around $\kappa = 0.2$ was noted and qualitatively discussed. The dependence on the β parameter (or inverse supercriticality) seems to be linear. The linear growth rate of the most unstable wave, when friction is taken into account, incorporates both β and κ, which are the only free parameters in our system. When PV flux is plotted against it, an approximate quadratic dependence appears, although the error of fit seems to be large.

More intense exploration of the parameter space seems appropriate to further establish any relationship of the eddy PV fluxes to the free parameters of the problem. A theory may be developed for PV flux parameterization in the framework of the truncated model once these relationships are more thoroughly studied. The reduced model could be possibly used either qualitatively, or quantitatively.

Acknowledgments

The constant guidance of Rick Salmon and Isaac Held, and the invaluable discussions we had throughout the summer are greatly appreciated. Thanks are due to the GFD program staff and all the visitors that constantly kept an intellectually stimulating atmosphere around Walsh Cottage. Last, but certainly not least, I'd like to thank my fellow Fellows for an unforgettable summer. I also gladly acknowledge the significant contribution of the beaches of Woods Hole, that were a true inspiration for hard work :-)

References

[1] R. Salmon, "Two-layer quasi-geostrophic turbulence in a simple case," Geophys. Astrophys. Fluid Dyn. **10**, 25 (1978).

[2] R. Salmon, "Baroclinic instability and geostrophic turbulence," Geophys. Astrophys. Fluid Dyn. **15**, 167 (1980).

[3] D. B. Haidvogel and I. M. Held, "Homogeneous quasi-geostrophic turbulence driven by a uniform temperature gradient," J. Atmos. Sci. **37**, 2644 (1980).

[4] R. L. Panetta and I. M. Held, "Baroclinic eddy fluxes in a one-dimensional model of quasi-geostrophic turbulence," J. Atmos. Sci. **45**, 3354 (1987).

[5] J. R. Holton, "A semi-spectral numerical model of wave-mean flow interactions in the stratosphere: Application to sudeen stratospheric warmings," J. Atmos. Sci. **33**, 1639 (1971).

[6] I. M. Held and M. J. Suarez, "A two-level primitive equation atmospheric model designed for climate sensitivity experiments," J. Atmos. Sci. **35**, 206 (1980).

[7] V. D. Larichev and I. M. Held, "Eddy amplitudes and fluxes in a homogeneous model of fully developed baroclinic instability," J. Phys. Ocean. **25**, 2285 (1995).

[8] I. M. Held and V. D. Larichev, "A scaling theory fo horizontally homogeneous, baroclinically unstable flow on a beta plane," J. Atmos. Sci. **53**, 946 (1996).

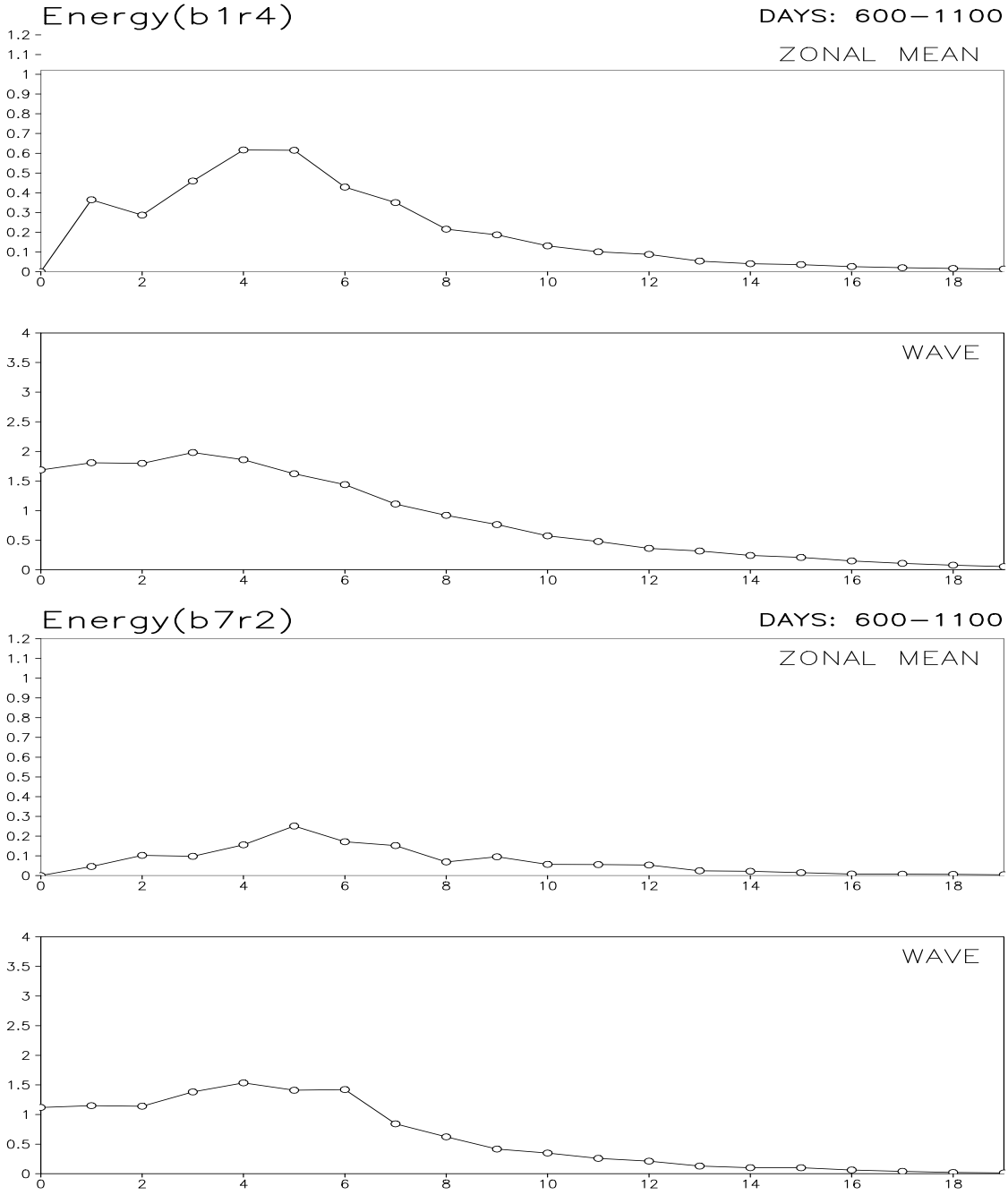

Figure 4: Energy spectra for two runs: top: $\beta = 0.05$, and $\kappa = 0.2$, bottom: $\beta = 0.35$, and $\kappa = 0.1$

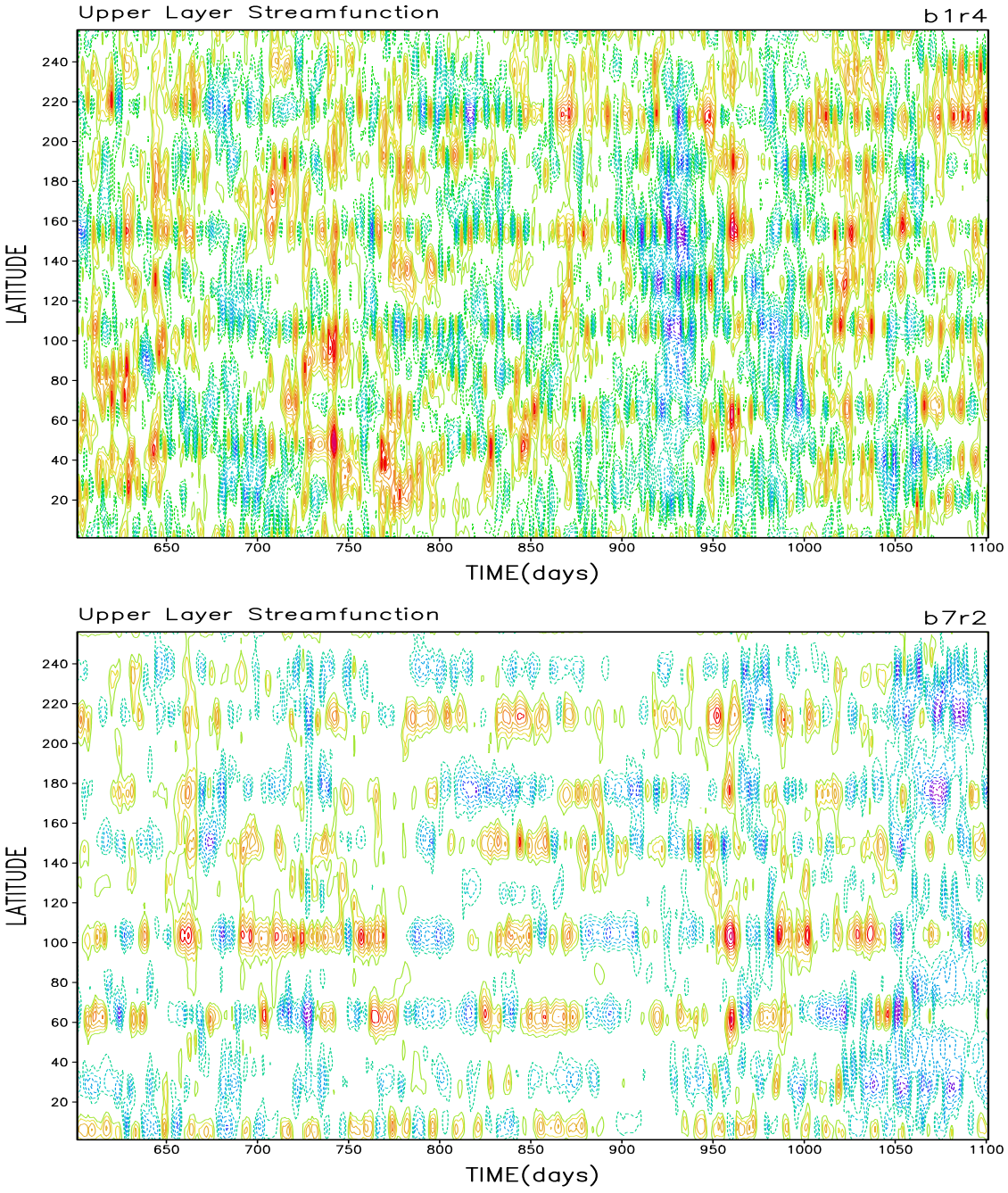

Figure 5: Hovmuller diagrams for two runs: top: $\beta = 0.05$, and $\kappa = 0.2$, bottom: $\beta = 0.35$, and $\kappa = 0.1$

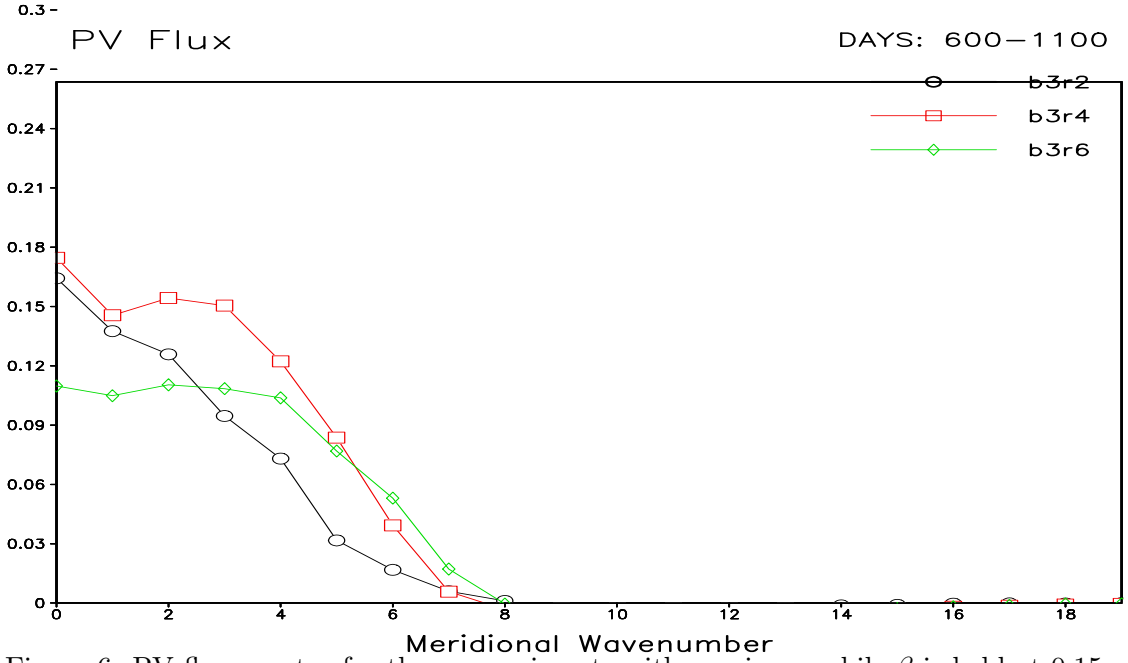

Figure 6: PV flux spectra for three experiments with varying κ while β is held at 0.15.

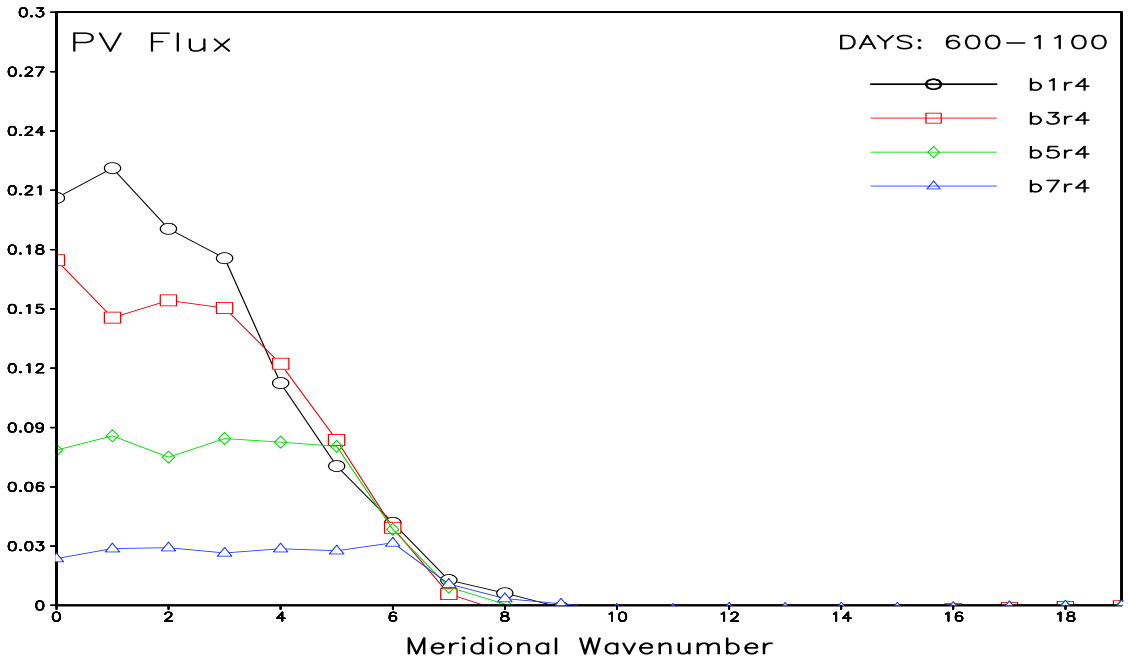

Figure 7: PV flux spectra for four experiments with varying β while the friction held at $\kappa = 0.2$.

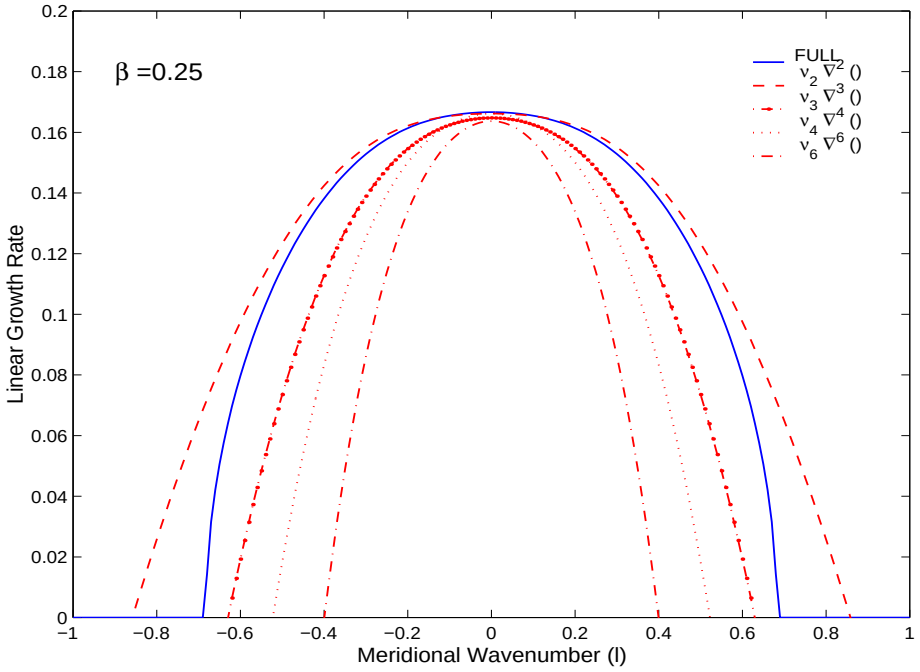

Figure 8: Linear growth rate as a function of meridional wavenumber (l) for the full model, and for the reduced model with modified eddy viscosity of degrees 2, 3, 4 and 6. β is set to 0.25

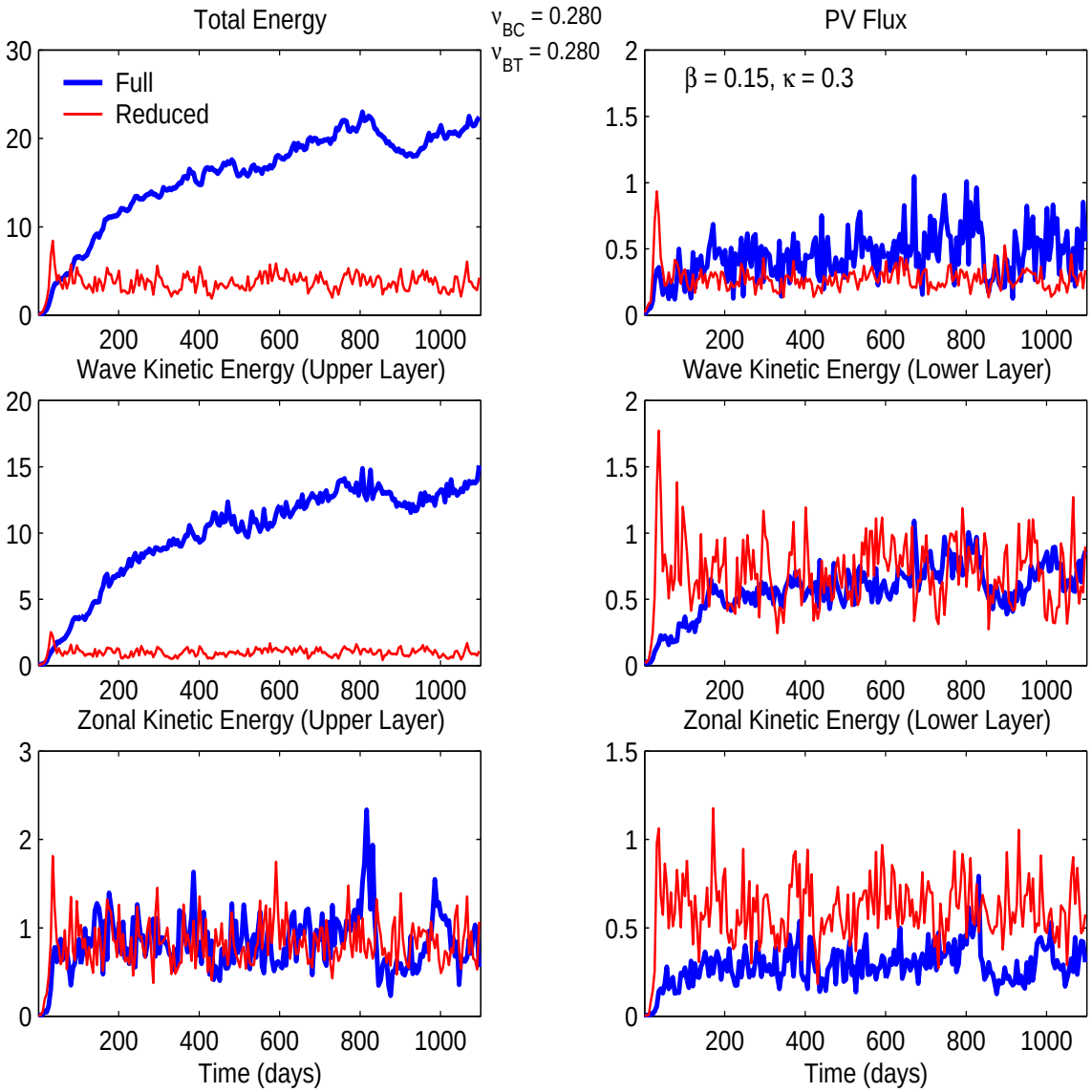

Figure 9: Total kinetic energy, PV flux, and kinetic energy of the zonal and wave components for the two layers for the full and the reduced models.

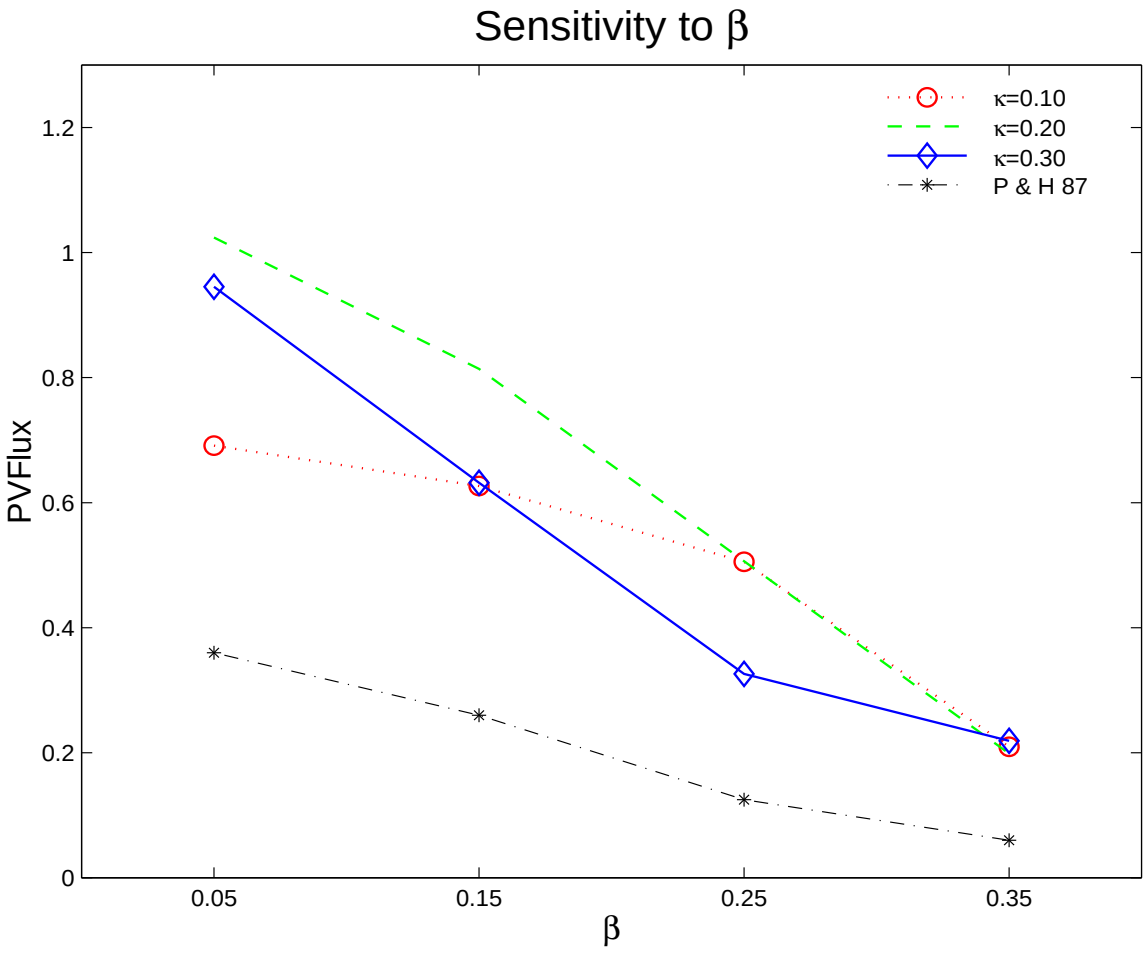

Figure 10: Time averaged behavior of equilibrated PV flux for varying β and κ instances. Results from [4] that include thermal damping are also included for comparison.

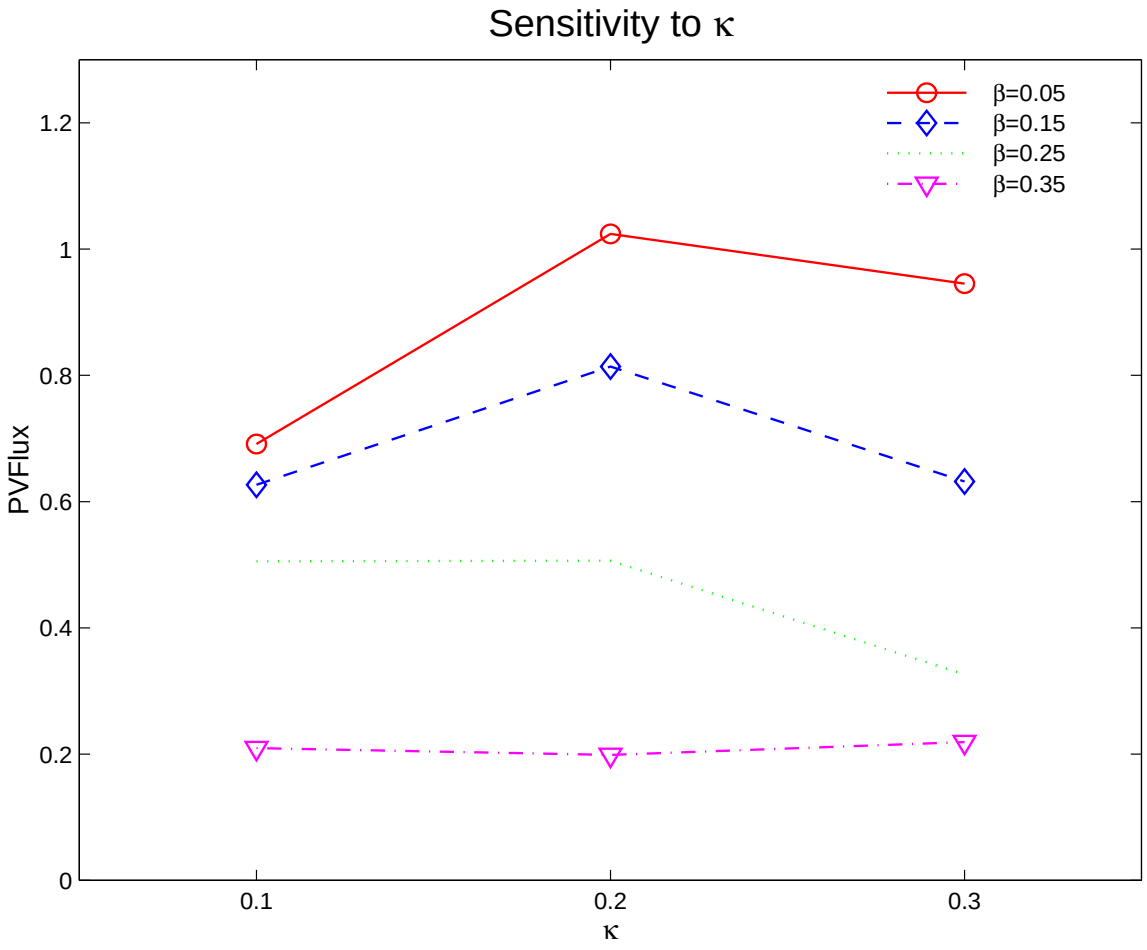

Figure 11: Time averaged behavior of equilibrated PV flux for varying β and three κ instances.

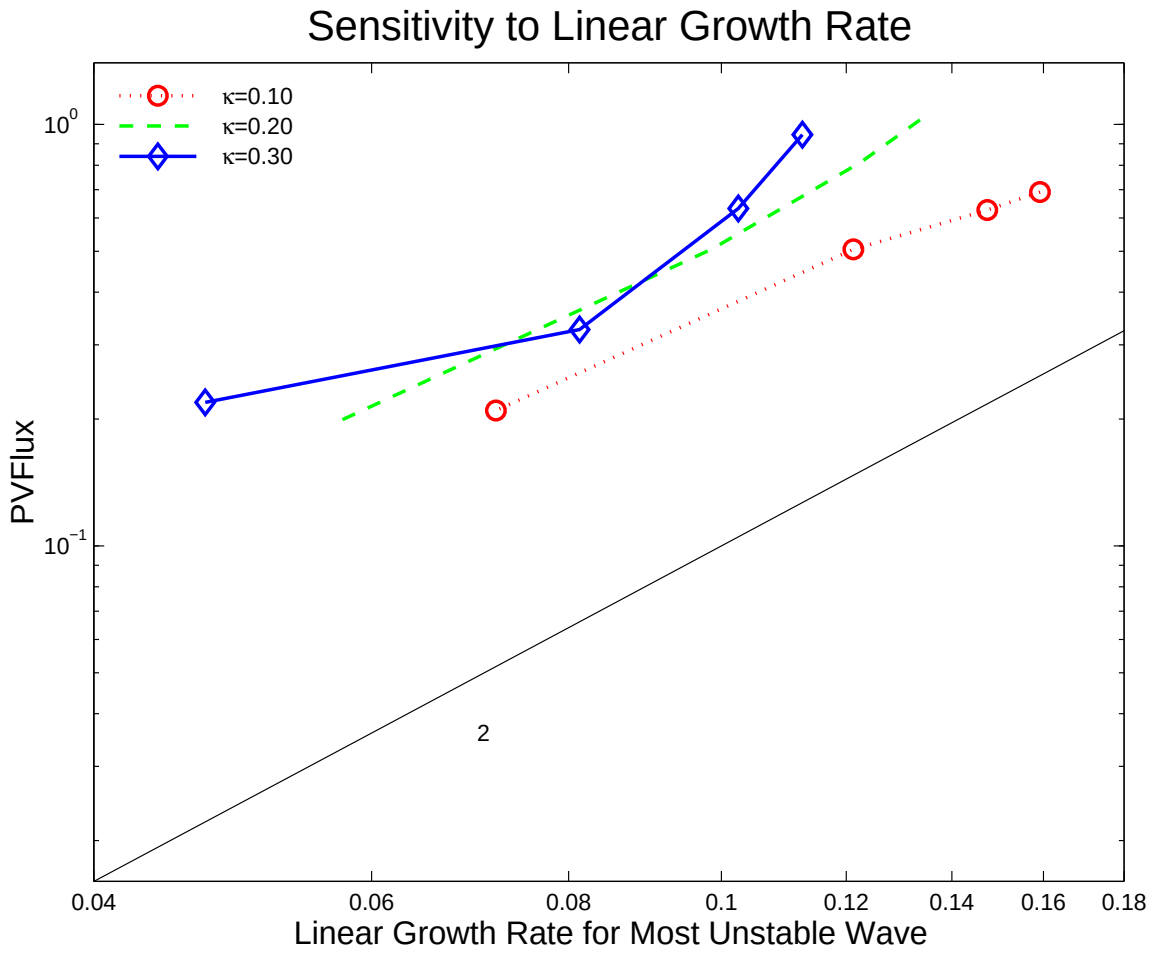

Figure 12: Time averaged behavior of equilibrated PV flux for varying and κ and β instances.